Biophysical Chemistry 300 (2023) 107075

Contents lists available at ScienceDirect

Biophysical Chemistry

journal homepage: www.elsevier.com/locate/biophyschem

DODAB vesicles containing lysophosphatidylcholines: The relevance of acyl chain saturation on the membrane structure and thermal properties

Letícia S. Martins [a], Evandro L. Duarte [b], M. Teresa Lamy [b], Julio H.K. Rozenfeld [a,*]

[a] Departamento de Biofísica, Escola Paulista de Medicina, Universidade Federal de São Paulo, R. Botucatu 862, São Paulo, SP 04023-062, Brazil
[b] Instituto de Física, Universidade de São Paulo, Rua do Matão 1371, São Paulo, SP 05508-090, Brazil

ARTICLE INFO

Keywords:
Dioctadecyldimethylammonium bromide
Lysophosphatidylcholine
Double bond
Membrane structure
Differential scanning calorimetry
Electron paramagnetic resonance spectroscopy

ABSTRACT

The saturated LPC18:0 and unsaturated LPC18:1 lysophosphatidylcholines have important roles in inflammation and immunity and are interesting targets for immunotherapy. The synthetic cationic lipid DODAB has been successfully employed in delivery systems, and would be a suitable carrier for those lysophosphatidylcholines. Here, assemblies of DODAB and LPC18:0 or LPC18:1 were characterized by Differential Scanning Calorimetry (DSC) and Electron Paramagnetic Resonance (EPR) spectroscopy. LPC18:0 increased the DODAB gel-fluid transition enthalpy and rigidified both phases. In contrast, LPC18:1 caused a decrease in the DODAB gel-fluid transition temperature and cooperativity, associated with two populations with distinct rigidities in the gel phase. In the fluid phase, LPC18:1 increased the surface order but, differently from LPC18:0, did not affect viscosity at the membrane core. The impact of the different acyl chains of LPC18:0 and 18:1 on structure and thermotropic behavior should be considered when developing applications using mixed DODAB membranes.

1. Introduction

Lysophosphatidylcolines (LPCs) are the most abundant type of lysolipids [1,2]. They are wedge-shaped surfactants formed by the enzymatic or oxidative hydrolysis of diacylphosphatidylcholines [2]. LPCs affect the curvature and elasticity of membranes, and are involved in membrane fusion processes [3]. They have also been used to prepare temperature sensitive liposomes [4].

Aside their surfactant activities, LPCs are important biological messengers involved in apoptosis [5], inflammation and immune responses [6] related to several pathologies, such as Chagas Disease [7], dementia [8], and acute liver failure [9]. Indeed, LPCs have been extensively investigated as biomarkers [2].

Among the most abundant LPCs in the human blood are the 18-carbon chain LPC18:0 and LPC18:1 [6]. The saturated LPC18:0 (Fig. 1) can protect against lethal experimental sepsis [10], possibly by inhibiting Caspase-11 activation [11]. Interestingly, LPC18:0 was recently shown to induce injury-associated pain [12]. Its unsaturated analog, LPC18:1, which has a *cis*-double bond (Fig. 1), was shown to stimulate the release of inflammatory cytokines by endothelial cells [5]. More importantly, LPC18:1 is able to activate NKT cells [13], and might help those cells monitor perturbations caused by oxidative stress [14]. Hence, these LPCs are interesting targets for developing novel immunotherapeutic tools.

Considering the multiple effects of LPCs, and the fact that their levels are regulated [2,6,14], the delivery of LPCs would be dependent on a suitable carrier. The synthetic cationic lipid dioctadecyldimethylammonium bromide (DODAB, Fig. 1) has been successfully used as a carrier and adjuvant for immunological applications [15,16]. Hence, DODAB membranes could be used to deliver LPCs.

The delivery efficiency is highly dependent on physicochemical properties such as charge, size, rigidity and hydrophobicity of the delivery system [17], therefore a structural characterization is required prior to biological application. Differential Scanning Calorimetry (DSC) provides information on how the organization of lipid systems is affected by temperature, and has been extensively employed to evaluate phase transitions in lipid membranes [18].

Electron Paramagnetic Resonance (EPR) spectroscopy is a technique that gives information about order and mobility of lipid membranes at different depths [19]. It is more sensitive than fluorescence spectroscopy to detect coexistence of different lipid phases and interdigitation [19], and has been widely used to characterize DODAB assemblies [19].

In this work, DSC and EPR spectroscopy were used to characterize the thermotropic behavior and structure of DODAB vesicles containing

* Corresponding author.
E-mail address: julio.rozenfeld@unifesp.br (J.H.K. Rozenfeld).

https://doi.org/10.1016/j.bpc.2023.107075
Received 18 May 2023; Received in revised form 28 June 2023; Accepted 2 July 2023
Available online 8 July 2023

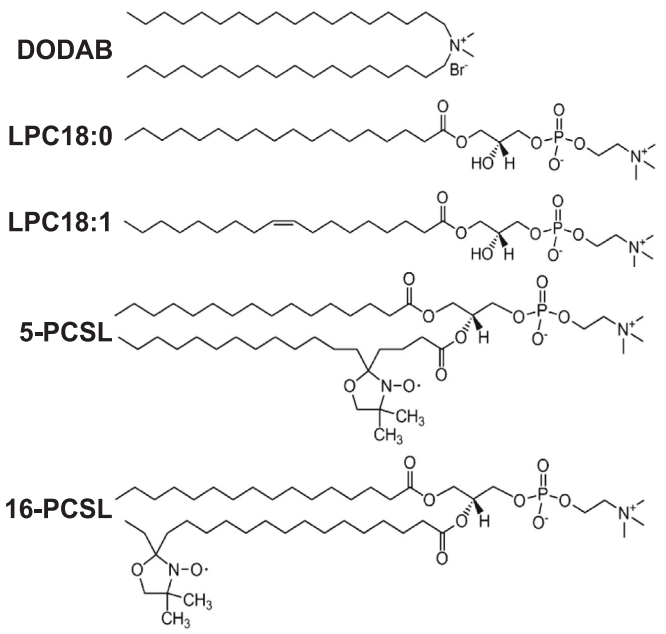

Fig. 1. Chemical structures of DODAB, LPC18:0, LPC18:1, 5-PCSl and 16-PCSL.

LPC18:0 and LPC18:1.

2. Materials and methods

2.1. Materials

Dioctadecyldimethylammonium bromide (DODAB) (catalog number D2779), 1-Stearoyl-2-Hydroxy-sn-Glycero-3-Phosphocholine (LPC18:0) (catalog number 855775P), 1-Oleoyl-2-Hydroxy-sn-Glycero-3-Phosphocholine (LPC18:1) (catalog number 845875P), paramagnetic probes 1-Palmitoyl-2-Stearoyl-(*n*-doxyl)-sn-Glycero-3-Phosphocholine (*n*-PCSL, $n = 5$ or 16) and HEPES buffer were purchased from Sigma Chemical Co. (St. Louis, MO, USA). Ultrapure water was used throughout.

The chemical structures of lipids and spin labels are shown in Fig. 1.

2.2. Vesicles preparation

The vesicles were prepared by hydrating lipid films above the phase transition temperature of DODAB. Briefly, chloroform solutions containing DODAB, LPC18:0, LPC18:1, or DODAB plus one of the LPCs were dried under a nitrogen stream and left under reduced pressure for 2 h. The resulting lipid films were then dispersed in HEPES buffer (10 mM, pH 7.4) by heating for 20 min at 70 °C in a water bath. Heating was accompanied by vortexing at every 5 min in order to produce large vesicles [20].

For EPR experiments, 0.8 mol% of 5-PCSL or 0.3 mol% of 16-PCSL were added to the chloroform solutions. Final DODAB concentration was 2 mM. Final LPCs concentration were 0.1 mM or 0.2 mM, which correspond, respectively, to 5 mol% and 9 mol% of the total lipid concentration.

2.3. Differential scanning calorimetry (DSC)

DSC thermograms were obtained in a Microcal VP-DSC Microcalorimeter (Microcal Inc., Northampton, MA, USA). Heating rates were 20 °C/h. Scans were performed with at least two samples prepared in different days. An annealing scan of 90 °C/h was performed prior to all experiments. Thermodynamic parameters such as the phase transition temperature (Tm), the phase transition enthalpy (ΔH), and the width at half-maximum ($\Delta T_{1/2}$) were obtained from analyses using the Microcal

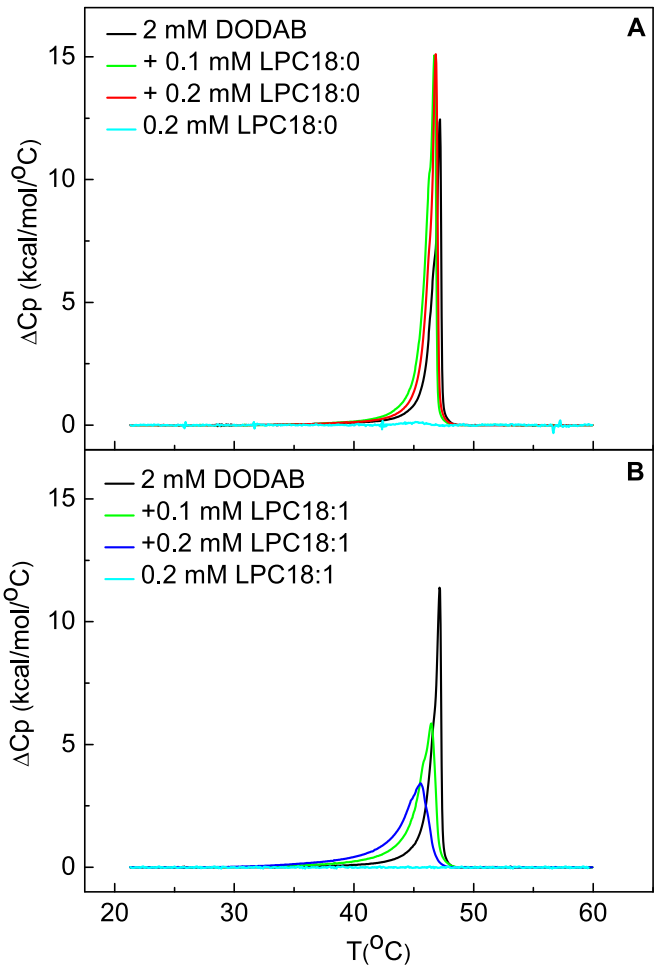

Fig. 2. Effect of LPC18:0 (A) and LPC18:1 (B) on the thermograms of 2 mM DODAB bilayers. Scan rate was 20 °C/h.

Origin software. Tm is the temperature at the maximum value of heat capacity (ΔCp) [21]. ΔH values are obtained by integrating the area under the thermograms, and represent the enthalpy changes per molecule of lipid [21]. $\Delta T_{1/2}$ is the temperature range (width) at half peak height, and is related to the phase transition cooperativity: if the transition is more cooperative, it takes a lower $\Delta T_{1/2}$ value to be completed [21,22].

2.4. Electron paramagnetic resonance (EPR) spectroscopy

A Bruker EMX spectrometer equipped with the ER4119HS high sensitivity cavity was used to obtain EPR spectra in the X band. The microwave power was 13.4 mW, the modulation frequency was 100 kHz, and the modulation amplitude was 1 G. Sample temperatures were kept within 0.1 °C using a Bruker BVT-2000 variable temperature device.

The values of maximum (Amax) and minimum (Amin) hyperfine splittings and those of the low (h_{+1}), central (h_0) and high (h_{-1}) field line amplitudes were measured directly from the spectra (see Figs. 3 and 5).

The effective order parameter, S_{eff}, was calculated from the expression [23]

$$S_{eff} = \frac{A_{\parallel} - A_{\perp}}{A_{zz} - (1/2)(A_{xx} + A_{yy})} \frac{a_o'}{a_o}$$

where $a_o' = (1/3)(A_{xx} + A_{yy} + A_{zz})$, $a_o = (1/3)(A_{\parallel} + 2A_{\perp})$, $A_{\parallel}$ $(= A_{max})$ is the maximum hyperfine splitting directly measured in the spectrum

Table 1
Thermodynamic parameters of 2 mM DODAB bilayers and their mixtures with LPC18:0 or LPC18:1.

	Tm[a] (± s.d.) (°C)	ΔH (± s.d.) (kcal/mol)	$\Delta T_{1/2}$ (± s.d.) (°C)
2 mM DODAB	47.1 ± 0.0	12.2 ± 0.3	0.7 ± 0.0
+ 0.1 mM LPC 18:0	46.7 ± 0.0	17.8 ± 0.1	0.8 ± 0.1
+ 0.2 mM LPC 18:0	46.8 ± 0.0	15.8 ± 0.1	0.7 ± 0.0
+ 0.1 mM LPC 18:1	46.3 ± 0.0	12.9 ± 0.1	1.6 ± 0.1
+ 0.2 mM LPC 18:1	45.6 ± 0.1	11.7 ± 0.2	2.3 ± 0.0

[a] Tm was considered as the highest ΔCp value.

(see Fig 5),

$A_{\perp} = A_{min} + 1.4\left[1 - \frac{A_{\parallel} - A_{min}}{A_{zz} - (1/2)(A_{xx} + A_{yy})}\right]$, A_{min} is the measured inner hyperfine splitting (see Fig. 5) and A_{xx}, A_{yy} and A_{zz} are the principal values of the hyperfine tensor for doxylpropane [24].

Each experiment was performed at least in duplicate and error values correspond to standard deviations.

3. Results

3.1. LPC18:1 decreases the gel-fluid transition temperature and cooperativity of DODAB membranes, whereas LPC18:0 increases the gel-fluid transition enthalpy

Thermograms of DODAB, LPC18:0, LPC18:1, and DODAB + LPCs dispersions are shown in Fig. 2.

Thermograms of 2 mM DODAB vesicles show a narrow endothermic peak around 47 °C (Fig. 2A,B). This narrow peak is characteristic of a cooperative gel-fluid transition, where conformational changes are transmitted between molecules resulting in a collective change of the molecular array [21], and has been described for diluted DODAB dispersions prepared in HEPES buffer [25–27].

In contrast, the thermograms of 0.2 mM LPC18:0 (Fig. 2A) and 0.2 mM LPC18:1 (Fig. 2B) do not show thermal events. Although the LPC concentrations tested are well above the critical micelle concentrations (CMCs) of both LPC18:0 (0.4 μM) [28] and LPC18:1 (3 μM - 5 μM) [29], they are still in a diluted regime where only micelles are present. At higher LPC concentrations, other phases and phase transitions have been described [30]. For instance, it was shown that LPC18:0 can present a lamellar to micellar transition for samples above 6 mM [31]. In this case, an endothermic peak around 27 °C is observed when samples are heated after incubation at 0 °C for long periods of time [31].

When LPC18:0 is mixed with DODAB, the membrane endothermic peak around 47 °C becomes more intense (Fig. 2A). On the other hand, when LPC18:1 is mixed, the DODAB gel-fluid transition peak is less intense, shifted to lower temperatures and broader (Fig. 2B). These changes in thermogram features result in changes of the thermodynamic parameters such as transition enthalpies (ΔH), phase transition temperatures (Tm) and widths at half-maximum of peaks ($\Delta T_{1/2}$), which are listed in Table 1.

Mixtures of DODAB and LPC18:0 present a slight decrease (less than 0.5 °C) in Tm value when compared to pure DODAB vesicles, and the $\Delta T_{1/2}$ values are very similar in these mixtures and pure DODAB vesicles (Table 1). The ΔH value is significantly increased when LPC18:0 is mixed with DODAB: the highest LPC18:0 concentration tested (0.2 mM) resulted in roughly a 30% increase in the transition enthalpy when compared to pure DODAB (Table 1).

On the other hand, the Tm value decreases as LPC18:1 concentration is increased in mixtures with DODAB, and the highest LPC18:1 concentration tested (0.2 mM) resulted in a 1.5 °C decrease in Tm (Table 1). The $\Delta T_{1/2}$ value has more than doubled when LPC18:1 is mixed with DODAB, indicating an important decrease in DODAB gel-fluid transition cooperativity (Table 1). The ΔH value does not significantly change when LPC18:1 is mixed with DODAB (Table 1).

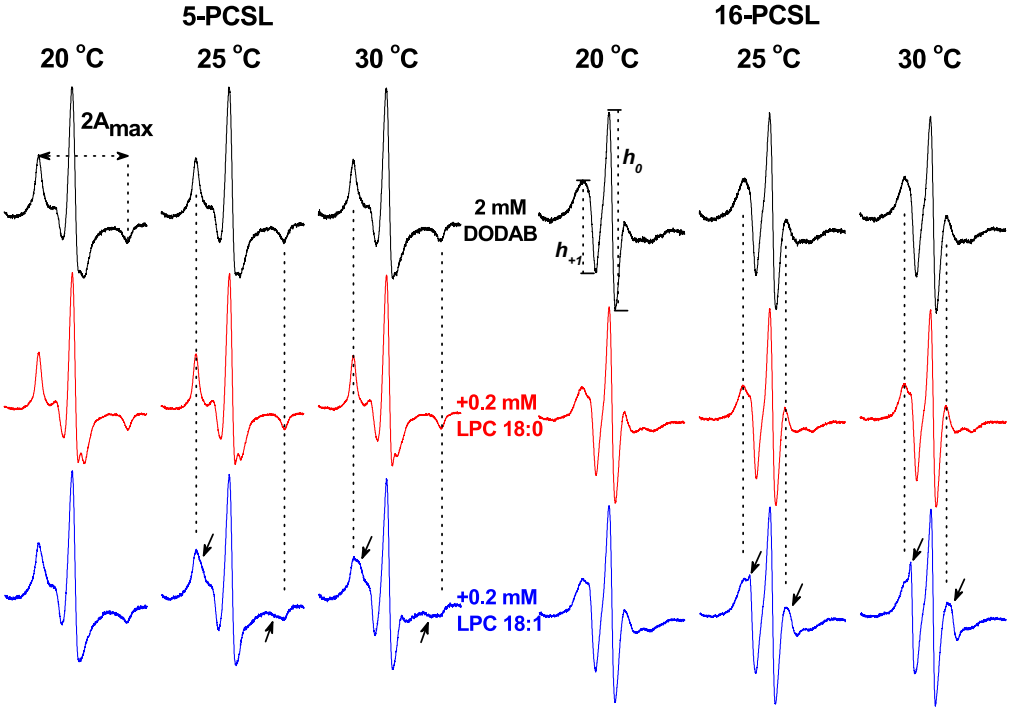

Fig. 3. Effect of LPC18:0 and LPC18:1 on the ESR spectra of 5-PCSL and 16-PCSL embedded in 2 mM DODAB bilayers in the gel phase. The maximum hyperfine splitting (Amax) and the amplitudes of low (h_{+1}) and central (h_0) field lines are indicated. The total spectra width is 100 G. Arrows indicate features of a more isotropic component and dotted lines indicate those typical of pure DODAB gel phase.

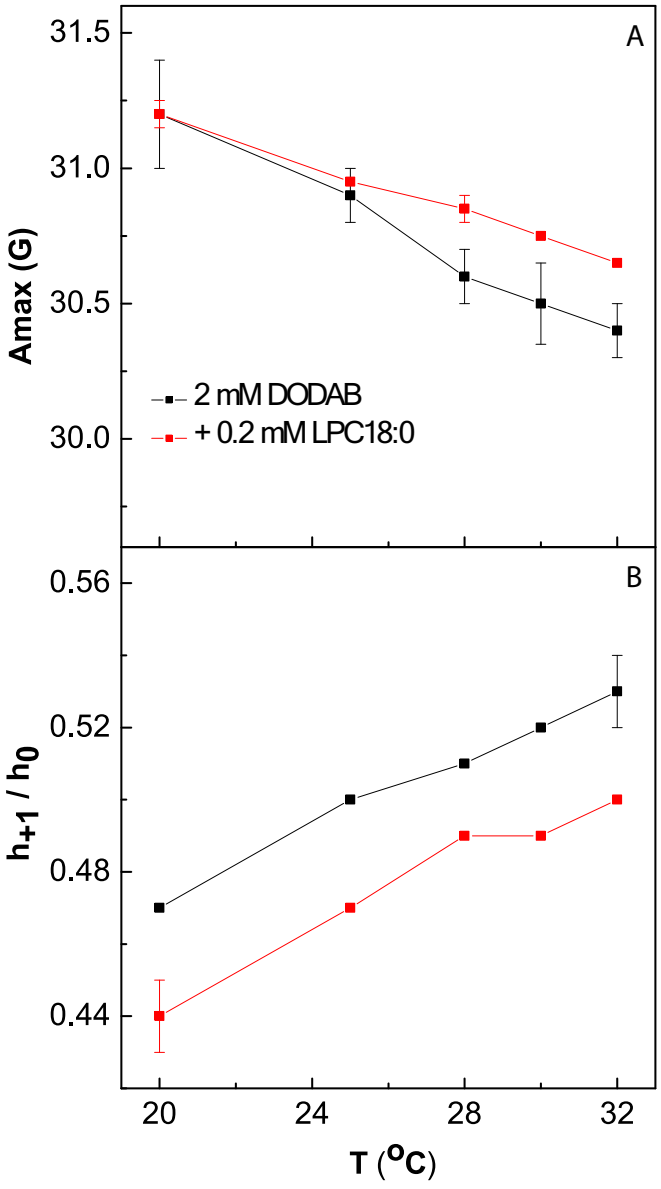

Fig. 4. Effect of LPC18:0 on the maximum hyperfine splitting (Amax) of 5-PCSL (A) and on the ratio of the low and central field line amplitudes (h_{+1} / h_0) of 16-PCSL (B) embedded in 2 mM DODAB bilayers at the gel phase. Error bars indicate standard deviations of at least two experiments with different samples.

3.2. LPC18:0 increases the rigidity of the DODAB gel phase, while two populations with different rigidities are observed in mixtures of LPC18:1 and DODAB in the gel phase

EPR spectroscopy was used to compared the structures of pure 2 mM DODAB vesicles and mixed vesicles containing 0.2 mM LPCs. This technique gives information on viscosity and packing at different depths of the membrane, depending on the paramagnetic probes employed [19]. For instance, 5-PCSL gives information about the region closer to the water interface, while 16-PCSL gives information about the membrane core (Fig. 1).

Fig. 3 shows the spectra of 5-PCSL and 16-PCSL embedded in pure and mixed vesicles at temperatures below the DODAB gel-fluid transition.

In pure DODAB vesicles at the same temperature, it is possible to observe that the EPR spectra of 5-PCSL and 16-PCSL are very different (Fig. 3). These differences are due to the fact that 5-PCSL is in a more packed environment than 16-PCSL, i.e., the spectrum of 5-PCSL indicate a more anisotropic microregion than that of 16-PCSL. It is known that gel phase DODAB vesicles have a flexibility gradient towards the bilayer core in the gel phase [26,27]. This flexibility gradient is also observed in presence of LPC18:0 or LPC18:1 (Fig. 3).

The spectra of pure DODAB vesicles and of mixtures of DODAB and LPC18:0 are very similar, so empirical parameters obtained from the spectra (Fig. 3) can give more information about their structure (Fig. 4). For instance, the maximum hyperfine splitting (Amax) is a useful parameter to evaluate viscosity and packing of gel phase bilayers, because the Amax values decrease as viscosity or packing decreases [19]. As expected, Amax values decrease as temperature increases, but the Amax values of mixed DODAB + LPC18:0 vesicles decrease less than the ones of pure DODAB (Fig. 4A). This suggests that LPC18:0 rigidifies the surface of DODAB vesicles.

The Amax values cannot be accurately determined from the spectra of 16-PCSL (Fig. 3), because they are more isotropic. Hence, the ratio of the low and central field line amplitudes (h_{+1}/h_0) provide more information on the bilayer structure, because h_{+1}/h_0 values increase as the membrane becomes less packed [19]. Fig. 4B shows that h_{+1}/h_0 values are higher for pure DODAB vesicles than for mixed DODAB + LPC18:0. This indicates that LPC18:0 also rigidifies the core of DODAB membranes.

In contrast to the spectra of DODAB + LPC18:0, the spectra of DODAB + LPC18:1 are different form the ones of pure DODAB vesicles (Fig. 3). In the spectra of mixed DODAB + LPC18:1, there are features of a more isotropic component which coexists with the typical DODAB gel phase signal (Fig. 3). This more isotropic component corresponds to a less rigid population detected by both paramagnetic probes, more evidently by 16-PCSL (Fig. 3). The presence of two components that cannot be separated hinders the empirical analyses of the spectra, because the values of empirical parameters represent an average of the environment that is being sensed by the paramagnetic probes in the dispersions.

3.3. LPC18:0 increases the rigidity of the core and the surface of DODAB fluid vesicles, while LPC18:1 increases only the order of their surface

Fig. 5 shows the spectra of 5-PCSL and 16-PCSL embedded in pure and mixed vesicles at temperatures above the DODAB gel-fluid transition.

As expected, the spectra features of 5-PCSL shown in Fig. 5 are thinner than the ones observed in the gel phase (Fig. 3), indicating a fast movement on the long axis of the probes that is characteristic of a fluid yet organized structure near the interfacial region [24]. Similarly, the spectra profiles of 16-PCSL in the fluid phase (Fig. 5) have sharper peaks than the ones observed in the gel phase (Fig. 3), indicating a nearly isotropic movement of the nitroxide group in the interior of the membrane, which is typical of the motional narrowing regime [24].

When comparing the EPR spectra in pure DODAB and mixed DODAB + LPC vesicles at the fluid phase, it is possible to recognize some differences such as the more anisotropic features of 5-PCSL in presence of LPC18:0 when compared to pure DODAB vesicles (Fig. 5). However, the overall spectra profiles of 5-PCSL and 16-PCSL in presence of LPCs are similar to the ones in pure DODAB vesicles, and the use of empirical parameters can be more informative (Fig. 6).

As shown in Fig. 5, the maximum and minimum hyperfine splittings (Amax and Amin) can be accurately determined in the 5-PCSL spectra. The values of these hyperfine splittings can be used to calculate the effective order parameter (S_{eff}), as detailed in Section 2.4. This parameter is used to evaluate the acyl chain order, although it also has contributions from the paramagnetic label mobility [32]. Seff values decrease as the membrane becomes less ordered [19], which is the case when temperature is increased. (Fig. 6A).

Fig. 6A shows that in presence of LPC18:0 or LPC18:1 the S_{eff} values are higher than the ones for pure DODAB vesicles, showing that both LPCs increase the order near the membrane surface in the fluid phase.

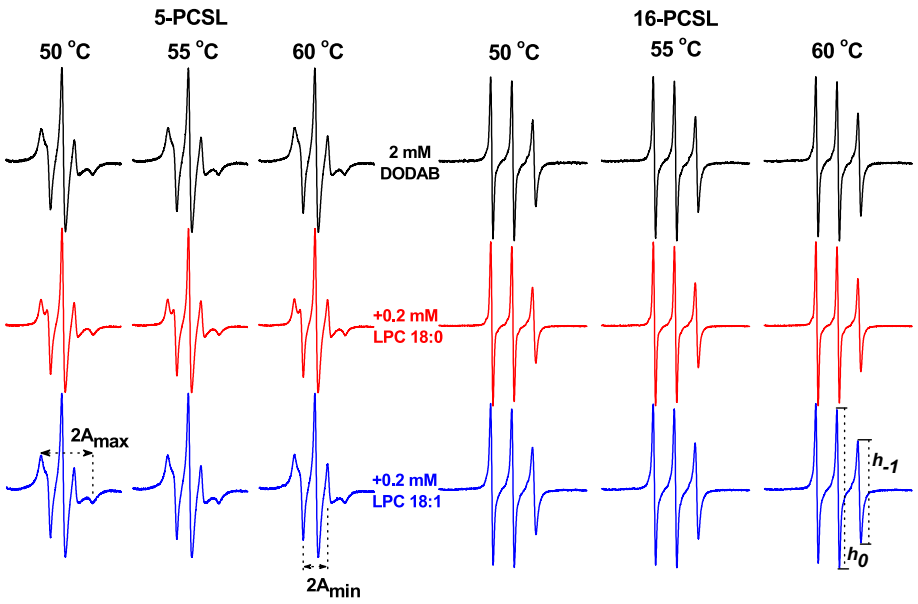

Fig. 5. Effect of LPC18:0 and LPC18:1 on the ESR spectra of 5-PCSL and 16-PCSL embedded in 2 mM DODAB bilayers in the fluid phase. The maximum (Amax) and minimum (Amin) hyperfine splittings and the amplitudes of high (h_{-1}) and central (h_0) field lines are indicated. The total spectra width is 100 G.

The nitroxide probe in16-PCSL is located deeper in the membrane (Fig. 1), and shows more isotropic spectrum that reflects a less ordered environment in the membrane core (Fig. 5). Hence, it is not possible to measure the hyperfine splittings from 16-PCSL spectra. In this case, the membrane viscosity or packing can be evaluated from the ratio of the amplitudes of the high (h_{-1}) and central (h_0) field lines (Fig. 5). Differently from S_{eff}, the h_{-1}/h_0 ratio increases as the membrane viscosity decreases [33], and this is the case for temperature increases (Fig. 6B).

In Fig. 6B, it is possible to observe that LPC18:0 decreases the h_{-1}/h_0 ratio at all temperatures, showing that it increases the DODAB membrane core viscosity at the fluid phase. In contrast, LPC18:1 does not affect the h_{-1}/h_0 ratio, suggesting that it does not affect the DODAB membrane core organization in the fluid phase (Fig. 6B).

In summary, Fig. 6 shows that LPC18:0 rigidifies the DODAB fluid phase both at the surface and in the core, whereas LPC18:1 only increases the surface order of the DODAB vesicles at the fluid phase.

4. Discussion

LPC18:0 does not alter the transition temperature and cooperativity of the DODAB gel-fluid transition, but significantly increases its ΔH values (Fig. 2 and Table 1). Increases in ΔH values have been described for alcohols [34] and anesthetics [35] that induce membrane interdigitation through interfacial effects. It was shown that pure LPC18:0 can form lamellar interdigitated structures at concentrations much higher than the ones tested here [31], as mentioned in Section 3.1. However, LPC18:0-induced interdigitation of DODAB bilayers can be outright discarded by the EPR spectra shown in Figs. 3 and 5, because the flexibility gradient of DODAB bilayers is maintained in presence of this LPC [36].

On the other hand, the empirical parameters obtained from these EPR spectra (Fig. 3) show that LPC18:0 increases the rigidity at the surface and core of the DODAB gel phase (Fig. 4). A similar effect is observed analyzing the empirical parameters of the fluid phase (Fig. 6). This increase in rigidity could explain the increase in ΔH values, which are dependent on headgroup interactions and hydration, as well as on acyl chains *trans-gauche* isomerism and Van der Waals interactions [37].

In agreement with that, LPC18:0 has a phosphatidylcholine headgroup that is polar and bulkier than the one of DODAB (Fig. 1), allowing a screening of the electrostatic repulsion between the cationic DODAB headgroups.

LPC18:0 also has a saturated 18-carbon acyl chain that perfectly matches the ones of DODAB, allowing an enhancement of Van der Waals interactions between the lipid chains (Fig. 1).

It was shown that the cone-shaped geometry of saturated LPCs enables their action as molecular harpoons that are able to sense and fit into hydrophobic defects of membranes [38]. DODAB membranes have many hydrophobic defects [39], that can even be observed by microscopy in the faceted aspect of gel phase giant unilamellar vesicles [40]. Hence, it is likely that LPC18:0 fits into these defects and increases both the gel (Fig. 4) and fluid (Fig. 6) phases packing.

In contrast to LPC18:0, LPC18:1 does not alter the ΔH values of the DODAB gel-fluid transition, but it decreases the transition temperature and cooperativity (Fig. 2, Table 1). A similar thermotropic behavior has been described for lipids that are completely miscible with DODAB, and was attributed to a destabilization of the DODAB gel phase by these lipids [26,27,40].

The EPR spectra of DODAB + LPC18:1 show two components, indicating the coexistence of a less rigid lipid population with the typical DODAB gel phase (Fig. 3). The presence of two signals that cannot be separated precludes the analysis of the empirical parameters, as explained in Section 3.2.

In order to test if the signals corresponding to the less rigid population could be due to the presence of LPC micelles, coexisting with DODAB + LPC vesicles, the spectra of 5-PCSL (Fig. S1) and 16-PCSL (Fig. S2) in pure LPCs were obtained at 30 °C, temperature in which the more isotropic signals are evident for both paramagnetic probes in Fig. 3. The spectra of spin labels incorporated in the micelles show broad and poorly defined peaks, and a baseline typical of the presence of spin-spin exchange [41] (Figs. S1 and S2). They confirm that 0.2 mM LPCs form micelles that are able to solubilize 5-PCSL and 16-PCSL, since these paramagnetic probes only exhibit an EPR signal when solubilized.

It is important to note, however, that the peaks corresponding to the LPC18:1 micelles are not in the same positions regarding the magnetic field intensity as the more isotropic components of DODAB + LPC18:1 mixtures (Fig. S3). This means that the signals of pure LPC18:1 micelles cannot be subtracted from the spectra of DODAB + LPC18:1 in order to obtain the spectra of pure DODAB, as previously described [42,43]. Consequently, the more isotropic signals observed for DODAB +

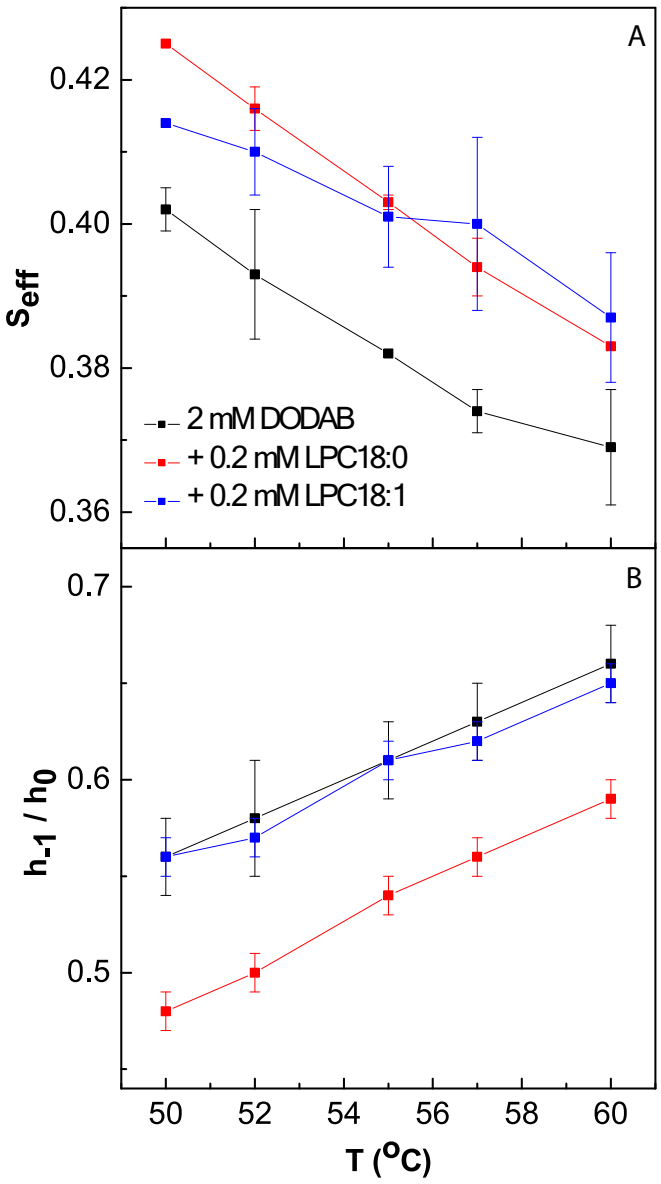

Fig. 6. Effect of LPC18:0 and LPC18:1 on the effective order parameter (S_{eff}) from 5-PCSL spectra (A) and on the ratio of the high and central field line amplitudes (h_{-1} / h_0) from16-PCSL spectra (B) embedded in 2 mM DODAB bilayers at the fluid phase. Error bars indicate standard deviations of at least two experiments with different samples.

LPC18:1 mixtures in Fig. 3 are not from pure LPC18:1 micelles.

It would also be possible that instead of pure LPC18:1 micelles, the more isotropic signals could be due to the presence of mixed DODAB + LPC18:1 micelles or bicelles. In this case, it would be expected a substantial decrease in ΔH values, as observed for DODAB bilayer fragments (bicelles) [44]. Considering that ΔH values remain unaltered in presence of LPC18:1 (Table 1), it is possible to discard the presence of mixed micelles or bicelles coexisting with LPC mixed DODAB vesicles.

From the discussion above, it is possible to conclude that the two populations observed in the EPR spectra of mixed DODAB membranes (Fig. 3) are a consequence of LPC18:1 molecules embedded in the DODAB gel phase. So far, only two works in the literature explore the interaction of LPC18:1 with gel phase membranes; they used NMR analyses to suggest that LPC18:1 is immiscible with DPPC in the gel phase, resulting in lateral phase segregation [45,46]. However, the decrease of the DODAB gel-fluid transition temperature, and the broadening of the transition (Fig. 2) are clear indications of the presence of LPC18:1 in DODAB gel phase.

Although lateral phase segregation could explain the presence of two populations in the EPR spectra (Fig. 3), it would also be expected to cause changes in the DSC thermograms. For instance, it was shown that the single endothermic peak of DSPC is split in two in presence of the immiscible lysolecithin [47]. Additionally, the anionic fatty acid oleic acid (OA) and the neutral glycerolipid monoolein (MO), which share the same 18-carbon unsaturated chain with LPC18:1, are completely miscible with DODAB vesicles well above 20 mol% [48,49], as shown by DSC and microscopy.

In any case, the presence of two populations detected by EPR would be consistent with a destabilization of the DODAB gel phase induced by LPC18:1. It is well known that *cis*-double bonds introduce a bend in the acyl chains that disturbs Van der Waals interactions and reduces transition temperatures and cooperativity [50]. Indeed, a similar gel phase destabilization was observed in mixtures of DODAB with MO [49] and with glycosphingolipids containing *cis*-double bonds in their ceramides [27,40].

Differently from the EPR spectra in the gel phase (Fig. 3), the spectra of DODAB + LPC18:1 in the fluid phase display a single population (Fig. 5), permitting empirical parameters to be obtained and analyzed (Fig. 6).

Similarly to LPC18:0, LPC18:1 increases the fluid DODAB membrane superficial order (Fig. 6A). The similar effect of both LPCs reinforces the idea that the membrane superficial order could be increased by the shielding of electrostatic repulsion between the small cationic DODAB headgroups by the polar and bulky phosphatidylcholine headgroup of LPCs.

On the other hand, LPC18:1 does not affect the viscosity at the membrane core (Fig. 6B), indicating that its *cis*-double bond does not disturb acyl chain mobility of fluid DODAB molecules, which have more freedom to wobble along the axis of the bilayer.

LPC18:0 and LPC18:1 have a single difference in their structure, which is the *cis*-double bond of the latter (Fig. 1). The present work shows that this difference has a significant impact on the effects these LPCs exert on the thermotropic behavior and structure of DODAB bilayers. It could also have a substantial impact on the use of these mixed bilayers in biotechnological applications.

It is possible that the rigidifying effect of LPC18:0 could be a disadvantage for the use of DODAB in delivery systems, because hydrophobic interactions facilitate the binding of many molecules, such as miconazole [51], gramicidin [52], DNA [53], and proteins [54], to DODAB membranes. Conversely, the apparent destabilization of the DODAB gel phase by LPC18:1 could be useful for applications in drug delivery for the reasons just mentioned. Indeed, MO, which has a *cis*-double bond like LPC18:1, was shown to improve the efficiency of DODAB as a DNA delivery system [55–57].

The immunological activity of LPC18:0 and LPC18:1 could also be affected or modulated by DODAB: it is known that liposomes of greater rigidity elicit higher antibody and cell-mediated immune responses [58]. Hence, the physicochemical characterization presented in this work could be important to develop new applications based on mixtures between DODAB and LPC18:0 or LPC18:1.

5. Conclusions

The thermotropic behavior and the structure of DODAB membranes containing LPC18:0 or LPC18:1 were characterized by DSC and EPR spectroscopy. LPC18:0 increased the DODAB gel-fluid transition enthalpy and rigidified both phases. This might be due to the screening of electrostatic repulsion of DODAB cationic headgroup by the phosphatidylcholine headgroup of LPC18:0, and by the enhancement of Van der Waals interactions between saturated acyl chains of DODAB and this lysolipid.

On the other hand, LPC18:1 caused a decrease in the DODAB gel-fluid transition temperature and cooperativity. This decrease is

consistent with a destabilization of the DODAB gel phase, which presents two populations with distinct rigidities in presence of LPC18:1. These effects are probably due to the *cis*-double bond of LPC18:1, which decreases the Van der Waals interactions between DODAB acyl chains. In the fluid phase, an increase in surface order was observed in presence of LPC18:1, possibly due to the electrostatic shielding of DODAB headgroups, as observed for LPC18:0. Interestingly, LPC18:1 did not affect viscosity at the DODAB fluid membrane core.

The difference in a single double bond between LPC18:0 and LPC18:1 resulted in a significant impact on how these lysolipids affect the thermotropic behavior and structure of DODAB membranes. These differences should be considered for the development of novel biotechnological applications using these mixed membranes.

Supplementary data to this article can be found online at https://doi.org/10.1016/j.bpc.2023.107075.

Author statement

I, Julio Rozenfeld, corresponding author, declare on my behalf and on behalf of all the coauthors that no Artificial Intelligence (AI) was employed during the production of this manuscript.

Declaration of Competing Interest

The authors declare the following financial interests/personal relationships which may be considered as potential competing interests.

Julio H K Rozenfeld reports equipment, drugs, or supplies was provided by Fapesp.

Acknowledgments

This work was supported by grants #2016/19077-1, #2016/13368-4, and #2021/01593-1, São Paulo Research Foundation (FAPESP). This study was financed in part by the Coordenação de Aperfeiçoamento de Pessoal de Nível Superior - Brasil (CAPES) - Finance Code 001. L.S.M. is supported by a CAPES PhD fellowship and M.T.L. is recipient of a CNPq research fellowship. From Brazil, the National Council for Scientific and Technological Development (CNPq - 465259/2014-6), the Coordination for the Improvement of Higher Education Personnel (CAPES), the National Institute of Science and Technology Complex Fluids (INCT-FCx), and the São Paulo Research Foundation (FAPESP - 2014/50983- 3).

References

[1] A. Grzelcyk, E. Gendaszewska-Darmach, Novel bioactive glycerol-based lysophospholipids: new data -new insight into their function, Biochimie 95 (2013) 667–679.
[2] K.M. Engel, J. Schiller, C.E. Galuska, B. Fuchs, Phospholipases and reactive oxygen species derived lipid biomarkers in healthy and diseased humans and animals – a focus on lysophosphatidylcholine, Front. Physiol. 12 (2021), 732319.
[3] L.V. Chernomordik, M.M. Kozlov, Mechanics of membrane fusion, Nat. Struct. Mol. Biol. 15 (2008) 675–683.
[4] B. Kneidl, M. Peller, G. Winter, L.H. Lindner, M. Hossann, Thermosensitive liposomal drug delivery systems: state of the art review, Int. J. Nanomedicine 9 (2014) 4387–4398.
[5] P. Liu, W. Zhu, C. Chen, B. Yan, L. Zhu, X. Chen, C. Peng, The mechanisms of lysophosphatidylcholine in the development of diseases, Life Sci. 247 (2020), 117443.
[6] S.T. Tan, T. Ramesh, X.R. Toh, L.N. Nguyen, Emerging roles of lysophospholipids in health and disease, Prog. Lipid Res. 80 (2020), 101068.
[7] M.A.C. Silva-Neto, A.H. Lopes, G.C. Atella, Here, there, and everywhere: the ubiquitous distribution of the immunosignaling molecule lysophosphatidylcholine and its role on Chagas disease, Front. Immunol. 7 (2016) 62.
[8] K. Phan, Y. He, R. Pickford, S. Bhatia, J.S. Katzeff, J.R. Hodges, O. Piguet, G. M. Halliday, W.S. Kim, Uncovering pathophysiological changes in frontotemporal dementia using serum lipids, Sci. Rep. 10 (2020) 3640.
[9] F.M. Trovato, R. Zia, F. Artru, S. Mujib, E. Jerome, A. Cavazza, M. Coen, I. Wilson, E. Holmes, A. Singanayagam, C. Bernsmeier, S. Napoli, W. Bernal, J. Wendon, R. Miquel, K. Menon, V.C. Patel, J. Smith, S.R. Atkinson, E. Triantafyllou, M.J. W. McPhail, Lysophosphatidylcholines modulate immunoregulatory checkpoints in peripheral monocytes and are associated with mortality in people with acute liver failure, J. Hepatol. 78 (2023) 558–573.
[10] G.Q. Chen, J.H. Li, X.L. Qiang, C.J. Czura, M. Ochani, K. Ochani, L. Ulloa, H. Yang, K.J. Tracey, P. Wang, A.E. Sama, H. Wang, Suppression of HMGB1release by stearoyl lysophosphatidylcholine: an additional mechanism for its therapeutic effects in experimental sepsis, J. Lipid Res. 46 (2005) 623–627.
[11] W. Li, W. Zhang, M. Deng, P. Loughran, Y. Tang, H. Liao, X. Zhang, J. Liu, T. R. Billiar, B. Lu, Stearoyl lysophosphatidylcholine inhibits endotoxin induced Caspase-11 activation shock, Shock 50 (2018) 339–345.
[12] D.A. Friston, J. Cuddihy, J. Luiz, A.H. Truong, L. Ho, M. Basra, P. Santha, O. Oszlacs, J.S. Valente, T. Marczylo, S. Junttila, H. Laycock, D. Collins, M. Vizcaychipi, A. Gyenesei, Z. Takats, G. Jancso, E. Want, I. Nagy, Elevated 18: 0 lysophosphatidylcholine contributes to the development of pain in tissue injury, Pain 164 (2023) e103–e115.
[13] J. Lopez-Sagaseta, L.V. Sibener, J.E. Kung, J. Gumperz, E.J. Adams, Lysophospholipid presentation by CD1d and recognition by a human natural killer T-cell receptor, EMBO J. 31 (2012) 2047–2059.
[14] L. Felley, J.E. Gumperz, Are human iNKT cells keeping tabs on lipidome perturbations triggered by oxidative stress in the blood? Immunogenetics 68 (2016) 611–622.
[15] J.H.K. Rozenfeld, S.R. Silva, P.A. Ranéia, E. Faquim-Mauro, A.M. Carmona-Ribeiro, Stable assemblies of cationic bilayer fragments and CpG oligonucleotide with enhanced immunoadjuvant activity *in vivo*, J. Control. Release 160 (2012) 367–373.
[16] L.R.M.M. Aps, M.B. Tavares, J.H.K. Rozenfeld, M.T. Lamy, L.C.S. Ferreira, M. O. Diniz, Bacterial spores as particulate carriers for gene gun delivery of plasmid DNA, J. Biotechnol. 228 (2016) 58–66.
[17] N. Benne, J. van Duijn, J. Kuiper, W. Jiskoot, B. Slütter, Orchestrating immune responses: how size, shape and rigidity affect the immunogenicity of particulate vaccines, J. Control. Release 234 (2016) 124–134.
[18] R.L. Biltonen, D. Lichtenberg, The use of differential scanning calorimetry as a tool to characterize liposome preparations, Chem. Phys. Lipids 64 (1993) 129–142.
[19] J.H.K. Rozenfeld, E.L. Duarte, T.R. Oliveira, M.T. Lamy, Structural insights on biologically relevant cationic membranes by ESR spectroscopy, Biophys. Rev. 9 (2017) 633–647.
[20] A.M. Carmona-Ribeiro, Synthetic amphiphile vesicles, Chem. Soc. Rev. 21 (1992) 209–214.
[21] J.T. Mason, Investigation of phase transitions in bilayer membranes, Methods Enzymol. 295 (1998) 468–494.
[22] A.G. Lee, Lipid phase transitions and phase diagrams I. lipid phase transitions, Biochim. Biophys. Acta Rev. Biomembr. 472 (1977) 237–281.
[23] J.M. Boggs, G. Rangaraj, Phase transitions and fatty acid spin label behavior in interdigitated lipid phases induced by glycerol and polymyxin, Biochim. Biophys. Acta Biomembr. 816 (1985) 221–233.
[24] W.L. Hubbell, H.M. McConnell, Molecular motion in spin-labeled phospholipids and membranes, J. Am. Chem. Soc. 93 (1971) 314–326.
[25] F.M. Linseisen, S. Bayerl, T.M. Bayerl, 2H-NMR and DSC study of DPPC-DODAB mixtures, Chem. Phys. Lipids 83 (1996) 9–23.
[26] L.S. Martins, E.L. Duarte, M.T. Lamy, J.H.K. Rozenfeld, Supramolecular organization of α-galactosylceramide in pure dispersions and in cationic DODAB bilayers, Chem. Phys. Lipids 232 (2020), 104963.
[27] L. Andrade, E.L. Duarte, M.T. Lamy, J.H.K. Rozenfeld, Thermotropic behavior and structural organization of C24:1 sulfatide dispersions and its mixtures with cationic bilayers, ACS Omega 8 (2023) 5306–5315.
[28] R.E. Stafford, T. Fanni, E.A. Dennis, Interfacial properties and critical micelle concentration of lysophospholipids, Biochemistry 28 (1989), 5113-51-20.
[29] N. Bergstrand, K. Edwards, Aggregate structure in dilute aqueous dispersions of phospholipids, fatty acids, and lysophospholipids, Langmuir 17 (2001) 3245–3253.
[30] G. Arvidson, I. Brentel, A. Khan, G. Lindblom, K. Fontell, Phase equilibria in four lysophosphatidylcholine/water systems. Exceptional behaviour of 1-palmitoyl-glycerophosphocholine, Eur. J. Biochem. 152 (1985) 753–759.
[31] F.G. Wu, N.N. Wang, J.S. Yu, J.J. Luo, Z.W. Yu, Nonsynchronicity phenomenon observed during the lamellar-micellar phase transitions of 1-stearoyllysophosphatidylcholine dispersed in water, J. Phys. Chem. B 114 (2010) 2158–2164.
[32] H. Schindler, J. Seelig, EPR spectra of spin labels in lipid bilayers, J. Chem. Phys. 59 (1973) 1841–1850.
[33] D. Marsh, in: L.J. Berliner, J. Reuben (Eds.), Spin Labeling. Theory and Applications 8, Plenum Press, New York, 1989, pp. 255–303.
[34] K.L. Griffin, C.Y. Cheng, E.A. Smith, P.K. Dea, Effects of pentanol isomers on the phase behavior of phospholipid bilayer membranes, Biophys. Chem. 152 (2010) 178–183.
[35] S.T. Reddy, S. Shrivastava, A. Chattopadhyay, Local anesthetics induce interdigitation and thermotropic changes in dipalmitoylphosphatidylcholine bilayers, Chem. Phys. Lipids 210 (2018) 22–27.
[36] J.H.K. Rozenfeld, E.L. Duarte, J.M. Ruysschaert, C. Lonez, M.T. Lamy, Structural characterization of novel cationic diC16-amidine bilayers: evidence for partial interdigitation, Biochim. Biophys. Acta Biomembr. 1848 (2014) 127–133.
[37] D. Marsh, General features of phospholipid phase transitions, Chem. Phys. Lipids 57 (1991) 109–120.
[38] E.A. Disalvo, L.I. Viera, L.S. Bakas, G.A. Senisterra, Lysophospholipids as natural molecular harpoons sensing defects at lipid membranes, J. Colloid Interface Sci. 178 (1996) 417–425.
[39] A.M. Carmona-Ribeiro, Interactions between charged spherical vesicles, J. Phys. Chem. 97 (1993) 11843–11846.
[40] L.S. Martins, D.A. Nomura, E.L. Duarte, K.A. Riske, M.T. Lamy, J.H.K. Rozenfeld, Structural characterization of cationic DODAB bilayers containing C24:1 β-glucosylceramide, Biochim. Biophys. Acta Biomembr. 1861 (2019) 643–650.

[41] P. Devaux, H.M. McConnell, Lateral diffusion in spin-labeled phosphatidylcholine multilayers, J. Am. Chem. Soc. 94 (1972) 4475–4481.
[42] C.R. Benatti, E. Feitosa, R.M. Fernandez, M.T. Lamy-Freund, Structural and thermal characterization of dioctadecyldimethylammonium bromide dispersions by spin labels, Chem. Phys. Lipids 111 (2001) 93–104.
[43] C.R. Benatti, R.M. Epand, M.T. Lamy, Low cholesterol solubility in DODAB liposomes, Chem. Phys. Lipids 145 (2007) 27–36.
[44] J.H.K. Rozenfeld, T.R. Oliveira, M.T. Lamy, A.M. Carmona-Ribeiro, Interaction of cationic bilayer fragments with a model oligonulceotide, Biochim. Biophys. Acta Biomembr. 1808 (2011) 649–655.
[45] C.J.A. Van Echteld, B. De Kruijff, J. De Gier, Differential miscibility properties of various phosphatidylcholine/lysophosphatidylcholine mixtures, Biochim. Biophys. Acta 595 (1980) 71–81.
[46] C.J.A. Van Echteld, B. De Kruijff, J.G. Mandersloot, J. De Gier, Effects of lysophosphatidylcholines on phosphatidylcholine and phosphatidylcholine/cholesterol liposome systems as revealed by ^{31}P-NMR, electron microscopy and permeability studies, Biochim. Biophys. Acta 649 (1981) 211–220.
[47] A. Blume, B. Arnold, H.U. Weltzien, Effects of a synthetic lysolecithin analog on the phase transition of mixtures of phosphatidylethanolamine and phsophatidylcholine, FEBS Lett. 61 (1976) 199–202.
[48] M. Kepczynski, J. Lewandowska, K. Witkowska, S. Kedracka-Krok, V. Mistrikova, J. Bednar, P. Wydro, M. Nowakowska, Bilayer structures in dioctadecyldimethylammonium bromide / oleic acid dispersions, Chem. Phys. Lipids 164 (2011) 359–367.
[49] M.S.C. Oliveira, J.P.N. Silva, E. Feitosa, E.F. Marques, E.M.S. Castanheira, M.E.C. D. Oliveira, Aggregation behavior of aqueous dioctadecyldimethylammonium bromide / monoolein mixtures: a multitechnique investigation on the influence of composition and temperature, J. Colloid Interface Sci. 374 (2012) 206–217.
[50] Z.Q. Wang, H.N. Lin, S. Li, C.H. Huang, Phase transition behavior and molecular structures of monounsaturated phosphatidylcholines: calorimetric studies and molecular mechanics simulations, J. Biol. Chem. 270 (1995) 2014–2023.
[51] L.F. Pacheco, A.M. Carmona-Ribeiro, Effects of synthetic lipids on solubilization and colloid stability of hydrophobic drugs, J. Colloid Interface Sci. 258 (2003) 146–154.
[52] C.A. Carvalho, C. Olivares-Ortega, M.A. Soto-Arriaza, A.M. Carmona-Ribeiro, Interaction of gramicidin with DPPC/DODAB bilayer fragments, Biochim. Biophys. Acta 1818 (2012) 3064–3071.
[53] I.S. Kikuchi, A.M. Carmona-Ribeiro, Interactions between DNA and synthetic cationic liposomes, J. Phys. Chem. B 104 (2000) 2829–2835.
[54] L.R. Tsuruta, W. Quintilio, M.H. Costa, A.M. Carmona-Ribeiro, Interactions between cationic liposomes and an antigenic protein: the physical chemistry of the immunoadjuvant action, J. Lipid Res. 38 (1997) 2003–2011.
[55] J.P.N. Silva, P.J.G. Coutinho, M.E.C.D.R. Oliveira, Characterization of monoolein-based lipoplexes using fluorescence spectroscopy, J. Fluoresc. 18 (2008) 555–562.
[56] J.P.N. Silva, I.M.S.C. Oliveira, A.C.N. Oliveira, M. Lúcio, A.C. Gomes, P.J. G. Coutinho, M.E.C.D.R. Oliveira, Structural dynamics and physicochemical properties of pDNA/DODAB:MO lipoplexes: effect of pH and anionic lipids in inverted non-lamellar phases versus lamellar phases, Biochim. Biophys. Acta 1838 (2014) 2555–2567.
[57] A.C.N. Oliveira, T.F. Martens, K. Raemdonck, R.D. Adati, E. Feitosa, C. Botelho, A. C. Gomes, K. Braeckmans, M.E.C.D.R. Oliveira, Dioctadecyldimethylammonium : Monoolein nanocarriers for efficient in vitro gene silencing, ACS Appl. Mater. Interfaces 6 (2014) 6977–6989.
[58] D.S. Watson, A.N. Endsley, L. Huang, Design considerations for liposomal vaccines: influence of formulation parameters on antibody and cell-mediated immune responses to liposome associated antigens, Vaccine 30 (2012) 2256–2272.